Spectrochimica Acta Part A: Molecular and Biomolecular Spectroscopy 128 (2014) 868–873

Contents lists available at ScienceDirect

Spectrochimica Acta Part A: Molecular and Biomolecular Spectroscopy

journal homepage: www.elsevier.com/locate/saa

Light harvesting over a wide range of wavelength using natural dyes of gardenia and cochineal for dye-sensitized solar cells

Kyung Hee Park [a], Tae Young Kim [b], Shin Han [c], Hyun Seok Ko [d], Suk Ho Lee [e], Yong Min Song [f], Jung Hun Kim [f], Jae Wook Lee [f,*]

[a] Research Institute of Advanced Engineering Technology, Chosun University, Gwangju 501-759, Republic of Korea
[b] Department of Environmental Engineering, Chonnam National University, Gwangju 500-757, Republic of Korea
[c] School of Applied Chemical Engineering, Chonnam National University, Gwangju 500-757, Republic of Korea
[d] Department of Advanced S/ Chemicals, Chonnam National University, Gwangju 500-757, Republic of Korea
[e] Green Energy Institute, Mokpo-Si 530-400, Republic of Korea
[f] Department of Chemical and Biochemical Engineering, Chosun University, Gwangju 501-759, Republic of Korea

HIGHLIGHTS

- Successive adsorption of gardenia and cochineal were investigated.
- Photovoltaic efficiencies were highly dependent on the adsorption mechanism.
- Adsorption kinetics of the dyes was obtained with a pseudo-second-order model.

GRAPHICAL ABSTRACT

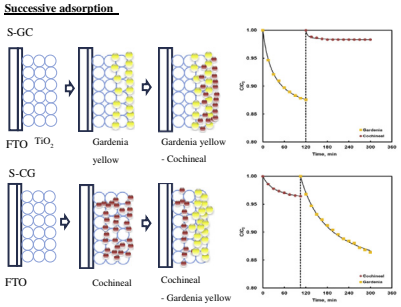

ARTICLE INFO

Article history:
Received 29 December 2013
Received in revised form 11 March 2014
Accepted 11 March 2014
Available online 24 March 2014

Keywords:
Light harvesting
Natural dyes
Double layers
Dye-sensitized solar cell
Photovoltaic performance

ABSTRACT

Two natural dyes extracted from gardenia yellow (*Gardenia jasminoides*) and cochineal (*Dactylopius coccus*) were used as sensitizers in the assembly of dye-sensitized solar cells (DSSCs) to harvest light over a wide range of wavelengths. The adsorption characteristics, electrochemical properties and photovoltaic efficiencies of the natural DSSCs were investigated. The adsorption kinetics data of the dyes were obtained in a small adsorption chamber and fitted with a pseudo-second-order model. The photovoltaic performance of a photo-electrode adsorbed with single-dye (gardenia or cochineal) or the mixture or successive adsorption of the two dyes, was evaluated from current–voltage measurements. The energy conversion efficiency of the TiO_2 electrode with the successive adsorption of cochineal and gardenia dyes was 0.48%, which was enhanced compared to single-dye adsorption. Overall, a double layer of the two natural dyes as sensitizers was successfully formulated on the nanoporous TiO_2 surface based on the differences in their adsorption affinities of gardenia and cochineal.

Introduction

Dye-sensitized solar cells (DSSCs) are composed of a nanoporous semiconductor oxide electrode, an adsorbed dye, and an electrolyte, and a counter electrode [1–4]. Many inorganic, organic, and hybrid dyes have been employed as sensitizers [5,6]. Because ruthenium dyes, including N719 and N3, are very expensive and environmentally toxic, numerous metal-free organic dyes have been applied as potential candidates in DSSCs [1,7]. Recently, several natural organic dyes such as anthocyanin, chlorophyll, tannin, and carotene extracted from various plants, fruits, flowers, and

* Corresponding author. Tel.: +82-62-230-7151.
E-mail address: jwlee@chosun.ac.kr (J. W. Lee).

http://dx.doi.org/10.1016/j.saa.2014.03.016
1386-1425/

leaves have been successfully used as sensitizers in DSSCs [8–15]. Research has focused on the easily available dyes extracted from natural sources and improved on efficiency, such as red yeast rice, seeweed, and chlorophyll include chlorin e-6. Ito et al. reported that a conversion efficiency of 2.3% was obtained using *Monascus Yellow* dye as sensitizer [16]. Chlorophyll is employed as sensitizer for DSSC with efficiency reported by Wang et al. as 4.6% [17]. Although natural dyes have many advantages of lower cost, color variety, and easy preparation compared to the synthetic ruthenium dyes, their energy conversion efficiencies are very low. To overcome this problem, some researchers have investigated dye-cocktail solutions which use two different dyes that absorb in lower and higher wavelength regions to capture light from the visible to the near IR, for the enhancement of DSSC performance [18–20]. The enhancement of DSSC performance using two or more dyes in such combinations has been reported. In random dye adsorption, unfavorable interactions between neighboring dye molecules cannot be avoided, which often leads to decreased photovoltaic performance. Therefore, it would be meaningful to compare the simultaneous and successive adsorption of the dyes to enhance both the adsorption amount and the electrochemical properties in the visible range. Recently, the successive adsorption of dyes had a significant advantage over dye-cocktails in overcoming the problem of unfavorable dye interactions [21].

The aim of this work was to study and optimize photovoltaic performance as a function of the adsorption characteristics and electrochemical properties of the dyes on TiO_2 thin films. To this end, adsorption kinetics data were obtained and analyzed by employing a pseudo-second-order model to understand the adsorption mechanisms of gardenia and cochineal mixtures, or the successive adsorptions of both dyes, for harvesting light over a wide range of wavelengths.

Experimental

Adsorption measurements

Gardenia dye is an evergreen fragrant flowering plant widely cultivated in gardens in South and East Asia [22,23]. The principal components of gardenia are crocin and crocetin (Fig. 1(a)). Cochineal dye is obtained from the dried bodies of females of the scale insect species, *Dactylopius coccus*, which feed on wild cacti [24]. The principal component of cochineal dye is carminic acid (Fig. 1(b)). Gardenia and cochineal were purchased from "the Naju Natural Dyeing Cultural Center" (Korea). All other chemical reagents were the guaranteed reagent grade. TiO_2 paste (DSL 18NR-T, Dyesol) was used to prepare TiO_2 films for the DSSCs. The paste was coated on pre-cleaned fluorine-doped SnO_2 conducting glass (FTO, Pilkington, TEC-8, 80% transmittance in the visible region) by a squeeze printing technique followed by annealing at 723 K for 30 min. A 10-μm-thick TiO_2 film was deposited on the 0.25 cm^2 FTO glass substrate. The adsorption kinetics experiments were carried out by immersing the TiO_2 cell with an active area of 4 cm^2 in a small adsorption chamber filled with an aqueous solution of gardenia and cochineal [25]. The amount of adsorption at time t (q_t) was calculated from Eq. (1):

$$q_t = (C_0 - C_t)V/W \quad (1)$$

where C_0 and C_t are the liquid phase concentrations (mg/L) of the natural dyes at the start and at any time, t, respectively. V is the volume of the solution, and W is the mass of adsorbent used. The concentrations of gardenia and cochineal were determined at 432 and 515 nm using a UV spectrophotometer (Shimadzu UV-160A, Japan) after filtration through a 0.015 μm UF membrane filter.

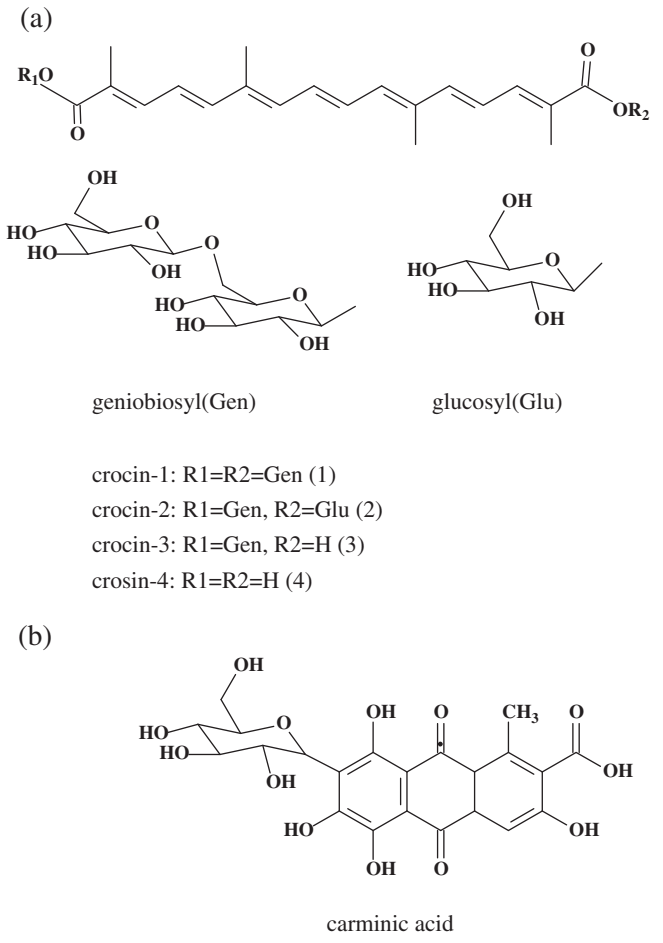

Fig. 1. Molecular structures of gardenia (a) and cochineal (b).

DSSC Fabrication

The adsorption of the gardenia and cochineal dyes was carried out by immersing a TiO_2 cell with an active area of 0.25 cm^2 into a 20 mL flask filled with an aqueous solution of the two natural dyes. A Pt-coated FTO (10 Ω/cm^2, Pilkington Co.) electrode was prepared as a counter electrode with an active area of 0.25 cm^2. The Pt-coated electrode was placed over the dye-adsorbed TiO_2 thin film electrode, and the edges of the cell were sealed with 5-mm-wide strips of 60-μm-thick sealing sheet (Meltonix 1170-60, Solaronix). Sealing was accomplished by hot-pressing the two electrodes together at 373 K. The redox electrolyte was injected into the cell through small holes, which were then sealed with a small square of sealing sheet. The redox electrolyte consisted of 0.3 M 1,2-dimethyl-3-propylimidazolium iodide (Solaronix), 0.5 M LiI (Aldrich), 0.05 M I_2 (Aldrich), and 0.5 M 4-tert-butylpyridine (4-TBP, Aldrich) and 3-methoxypropionitrile (3-MPN, Fluka) as a solvent.

Photoelectrochemical measurements

The capacities of the fabricated DSSCs and the current–voltage (I–V) curves were measured using a source measure unit under irradiation of white light from a 200 W Xenon lamp (McScience, Korea). The incident light intensity and the active cell area were 100 mW/cm^2 and 0.25 cm^2, respectively. The J–V curves were used to calculate the short-circuit current density (J_{sc}), open circuit photovoltage (V_{oc}), fill factor (FF), and overall conversion efficiency

(η_{eff}) of the DSSCs. Electrochemical impedance spectroscopy (EIS) measurements were performed using alternating current (AC) impedance (CHI 660A Electrochemical Work-station, USA) over the frequency range 1–10^6 Hz with amplitudes of ±5 mV over the V_{oc}.

Results and discussion

Fig. 2 shows photographic images and the UV–Vis absorption spectra of the gardenia and cochineal dyes dissolved in aqueous solution. A clear difference in the absorption characteristics of gardenia and cochineal dyes was observed. The absorption maximum for the gardenia extract was observed at a wavelength of approximately 441 nm, and those of cochineal at approximately 515 and 544 nm. Therefore, DSSCs adsorbed with both the gardenia and cochineal dyes could potentially be very effective for harvesting light over a wide range of wavelengths, resulting in higher photovoltaic conversion efficiency.

Recently, it was observed that the photovoltaic conversion efficiency was highly influenced by the adsorption characteristics of dye molecules and the electrochemical properties of the TiO_2 electrode. Therefore, it would be very meaningful to systematically examine the adsorption characteristics of the dyes on the TiO_2 films. Many studies of adsorption equilibria and kinetics have been conducted based on the differences in the amount of dye adsorbed and subsequently desorbed on TiO_2 thin films. However, as described in the experimental section, the adsorption kinetics data were directly obtained in a small adsorption chamber in the absence of the desorption step. The adsorption kinetics of gardenia and cochineal dyes on the TiO_2 film from aqueous solutions were obtained and then analyzed by employing a pseudo-second-order model. Kinetics data provide valuable information for

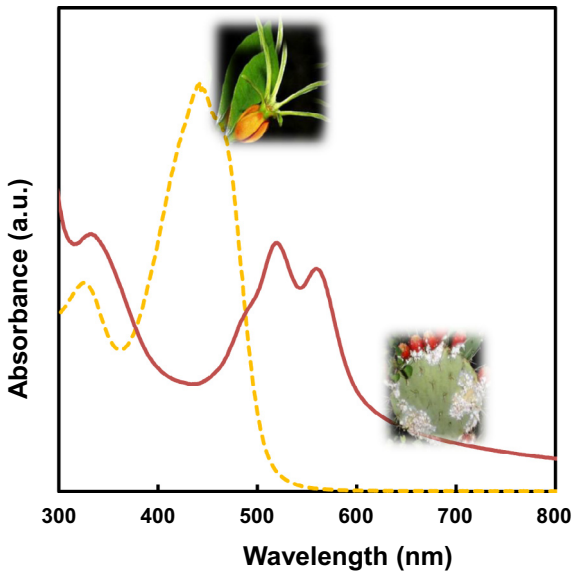

Fig. 2. UV–Vis absorption spectra of gardenia (yellow dot) and cochineal (red line) dyes.

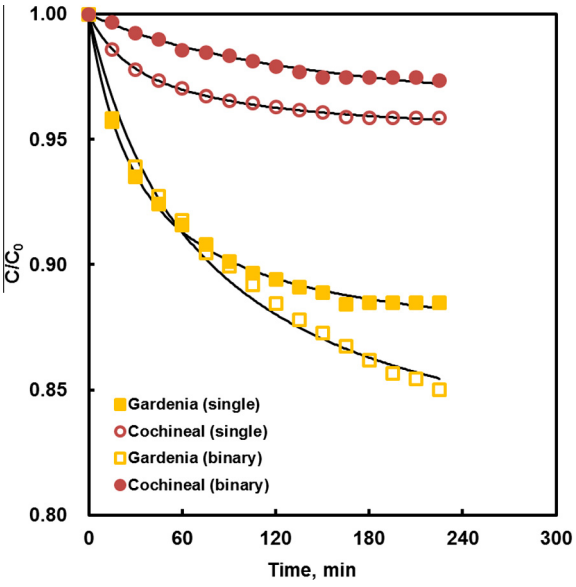

Fig. 3. Adsorption kinetics of single and binary dyes of gardenia and cochineal on TiO_2 electrodes.

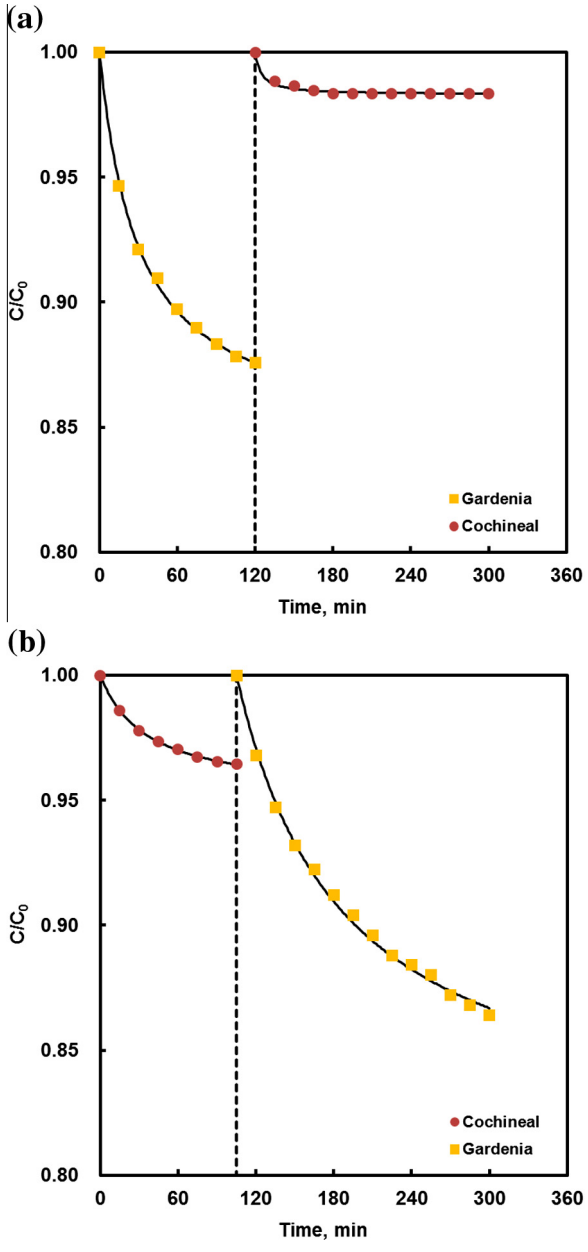

Fig. 4. Successive adsorption kinetics of S-GC (a) and S-CG (b).

understanding the mechanism of the sorption process [26]. Fig. 3 shows the obtained concentration decay curves of single-component adsorption of gardenia and cochineal on the TiO_2 film obtained in a small adsorption chamber. The solid lines are the simulated results using the kinetics model. The initial dye concentration and temperature were 450 mg/L and room temperature, respectively. The pH was not controlled. With increasing time, the amount of the adsorbed gardenia and cochineal dyes gradually increased. The adsorption affinity of gardenia involving the anchorage of the hydroxyl groups of the dye on the TiO_2 film surface was much greater than that of cochineal.

Recently, the Hayase group reported that DSSCs prepared by the adsorption of two dye mixtures effectively increased the efficiency. However, unfavorable interactions between the two dye molecules often decreased the photovoltaic performance. It is well-known that competitive adsorption generally occurs between binary components on the TiO_2 film during the progress of adsorption, in contrast to single component adsorption. Fig. 3 shows the concentration decay curves obtained in a small adsorption chamber for binary adsorption of gardenia and cochineal dyes (i.e., cocktail solution) on the TiO_2 film. As expected, the adsorption of either of these two dyes is influenced by the other component. The adsorption capacity of gardenia was 345 mg/g, and that of cochineal was 50 mg/g.

To understand the adsorption mechanism, the two successive adsorption cases were also employed: adsorption of gardenia followed by cochineal (S-GC) and adsorption of cochineal followed by gardenia (S-CG). Fig. 4 shows the interesting results that were observed for the adsorption process of S-GC and S-CG for the dye-bilayer formation. The interesting results can be observed for dye double layer formation from the S-GC and S-CG. Fig. 4(b) shows the adsorption of cochineal and followed by adsorption of gardenia on the same TiO_2 film. In this case, cochineal dye adsorbed at the TiO_2 surface was gradually replaced by gardenia. However, the S-GC sample showed that gardenia adsorbed on the TiO_2 surface was not replaced by cochineal because of the latter's lower adsorption affinity on TiO_2 films (Fig. 4(a)). The adsorption affinity of gardenia was higher than that of cochineal. However, the rate of adsorption of cochineal on the nanoporous TiO_2 surface is faster than that of gardenia which could be attributed to its smaller molecular size leading to higher diffusion through the nanoporous layer. Therefore, from the results of S-GC and S-CG results, the amounts of gardenia and cochineal adsorbed on the nanoporous TiO_2 surface can be successfully controlled based on the adsorption equilibria and kinetics differences of the two dyes. In other words, it is possible to adsorb two dyes in a dye double-layer architecture by successive adsorption, if we select one dye having faster adsorption and weaker binding with TiO_2 while the other dye has relatively slower diffusion along with stronger binding (Fig. 5).

The kinetics data were analyzed with a pseudo-second-order model [23,25].

$$dq/dt = k_2(q_e - q)^2 \quad (2)$$

where k_2 (g/mg/min) is the second-order rate constant determined by the plot of t/q_t vs. t. Note that the correlation coefficients (R^2) of the pseudo-second-order model for the linear plots of TiO_2 were very close to 1. This result implies that the adsorption kinetics was successfully described by the pseudo-second-order model. As listed in Table 1, the determined rate constants of q_e and k_2 were in the ranges 34–466 mg/g and 0.03–6.09 g/mg/min, respectively. In the case of the adsorption of gardenia and successive adsorption of cochineal on the same TiO_2 film, the adsorption capacity of former was 372 mg/g, and the latter was 34 mg/g. On the other hand, for the adsorption of cochineal and successive adsorption of gardenia on the same TiO_2 film, the gardenia adsorption capacity was 466 mg/g.

It is interesting to compare the influence of the adsorption mode on nanoporous TiO_2 surface (i.e., cocktail or successive adsorption) on the harvesting of light over a wide range of wavelengths. The photovoltaic parameters obtained by measuring I–V curves (Fig. 6) are listed in Table 2. The energy conversion efficiencies of the single-dye-sensitized solar cells using gardenia and cochineal were 0.35% and 0.10%, respectively. Contrary to our expectation, the mixture of the two dyes (i.e., cocktail DSSCs) showed decreased photovoltaic conversion efficiency because of

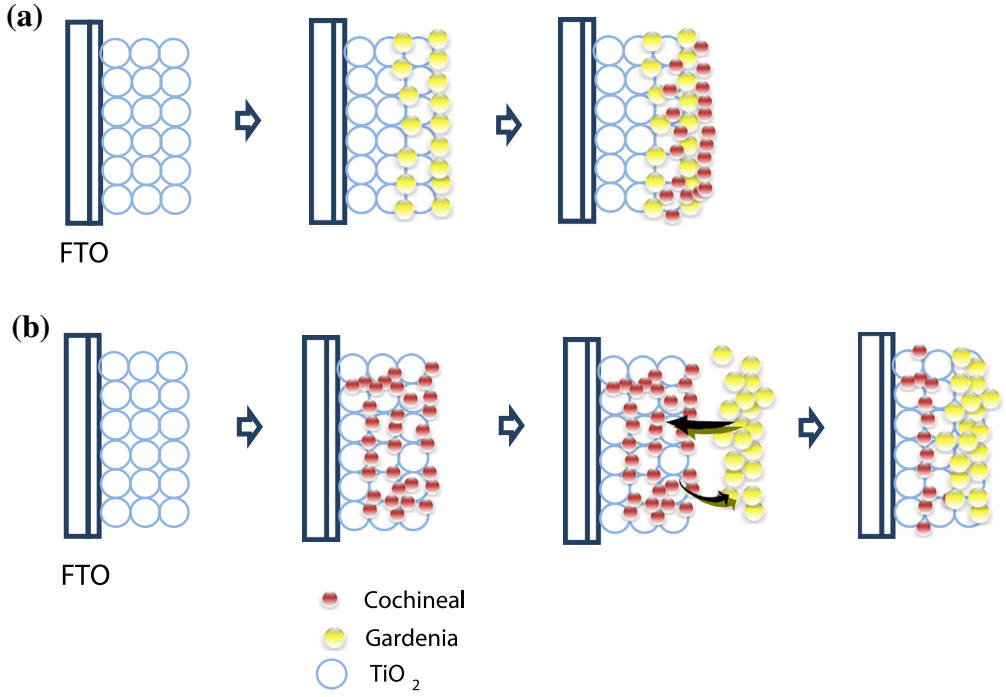

Fig. 5. Schematic explanations of successive adsorption of gardenia and cochineal on TiO_2 film for S-GC (a) and S-CG (b).

Table 1
The pseudo-second-order kinetic parameters of gardenia and cochineal adsorption on TiO_2 film.

Dyes		Pseudo-second-order-kinetics		
		q_e (mg/g)	k_2 (g/mg/min)	R^2
Gardenia	G	355	0.04	0.99
Cochineal	C	108	0.23	1.00
S-GC	G	372	0.09	1.00
	C	34	6.09	1.00
S-CG	C	104	0.27	1.00
	G	466	0.03	0.99
GC-cocktail	G	345	0.08	1.00
	C	50	0.12	0.93

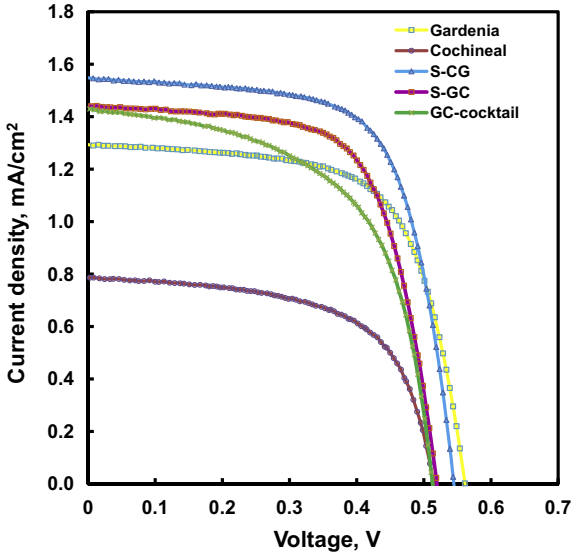

Fig. 6. Photocurrent–voltage curves of DSSCs adsorbed with GC-cocktail, S-CG and S-GC dyes.

the unfavorable interactions between the two dyes [20]. However, the S-CG solar cell yielded a short-circuit current density (J_{sc}) of 1.55 mA/cm^2, an open circuit photovoltage (V_{oc}) of 0.54 V, and a fill factor (FF) of 0.57, corresponding to a higher energy conversion efficiency (η) of 0.48%. To investigate the factors responsible for the improvement in cell performance, we carried out the impedance analysis to investigate their internal resistance properties. The EIS fitting results are shown in Fig. 7 and the analyzed data are summarized in Table 3. Generally, the DSSC spectra exhibited two or three semicircles, which were assigned to the electrochemical reaction at the Pt counter electrode, charge transfer at the TiO_2/dye/electrolyte, and the Warburg diffusion process of I^-/I_3^- [26]. Fig. 7 shows the fitted EIS data obtained with Z-View software using an equivalent circuit. The circuit elements comprised the interface charge-transfer resistance (R_{ct}), constant phase element

Table 2
Energy conversion efficiency of gardenia, cochineal, S-CG, S-GC and GC-cocktail dyes.

Dyes	V_{oc} (V)	J_{sc} (mA/cm^2)	FF	η (%)
Gardenia	0.56	1.29	0.48	0.35
Cochineal	0.51	0.78	0.25	0.10
S-CG	0.54	1.55	0.57	0.48
S-GC	0.52	1.44	0.50	0.37
GC-cocktail	0.51	1.43	0.43	0.31

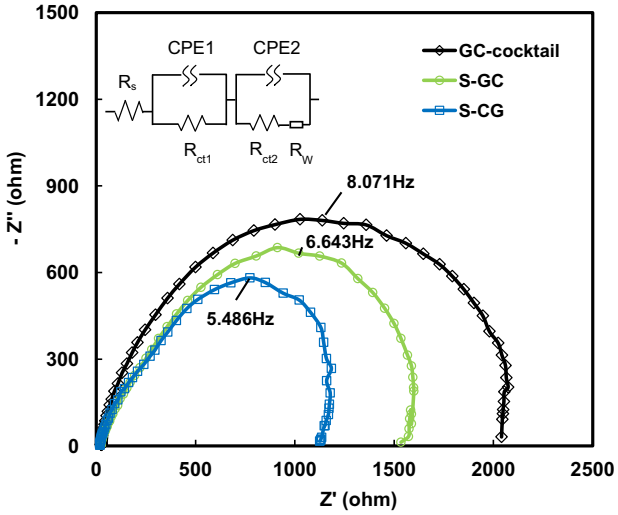

Fig. 7. The equivalent circuit and electrochemical impedance spectra of TiO_2 films adsorbed with S-GC, S-CG and GC-cocktail.

Table 3
Internal resistance of the cells by impedance analysis.

	R_s (Ω)	R_{ct1} (Ω)	R_{ct2} (Ω)
GC-cocktail	24	130	1138
S-CG	17	93	774
S-GC	22	108	912

(CPE), Warburg impedance (R_w), and series resistance (R_s). The R_{ct1} is the electron transfer resistance at the Pt/electrolyte interface, and the R_{ct2} is the electron transfer resistance at the TiO_2/dye/electrolyte interface. The CPE reflects the interfacial capacitance, taking into account the roughness of the electrodes, which causes depression of the semicircle to an ellipse in the Nyquist plots [27]. Compared with R_s of 24 Ω, 17 Ω, and 22 Ω for three cells, they showed similar R_s values as expected. However, R_{ct1} and R_{ct2} were significantly different. The R_{ct1} values were obviously reduced from 130 Ω of the GC-cocktail to 93 Ω of the S-CG. The trend correlated with the performance of the cells. The cell with the GC-cocktail as sensitizer had an obviously higher R_{ct2} (1138 Ω) than those of S-CG (774 Ω) and S-GC (912 Ω). The difference in R_{ct2} can be associated with the binding between the natural dye molecules and TiO_2 because the two main dyes in the gardenia and cochineal extracts aggregated or mixed together on the TiO_2 films, and thus, led to weaker binding and higher resistance. The high R_{ct2} led to decreases in the J_{sc}. This also may explain why the efficiency of the cell obtained from the GC-cocktail was so low. Therefore, in order to improve efficiency, it is necessary to improve the binding strength between natural dyes and nanoporous TiO_2 surfaces.

Conclusions

The adsorption properties of photoelectrodes that had adsorbed either a single dye (gardenia or cochineal), or a mixture of the two dyes were compared with respect to electron generation and electron transfer. The energy conversion efficiency in terms of adsorption mode (i.e., successive or cocktail adsorption) was in the range 0.10–0.48%. The conversion efficiency of the TiO_2 electrode with S-CG was 0.48%, which was enhanced compared to single-dye adsorption. The amounts of gardenia and cochineal dyes adsorbed on the nanoporous TiO_2 surface could be successfully controlled

based on the adsorption equilibria and kinetics differences of two dyes. The cochineal dye adsorbed faster with weak binding to TiO_2, whereas the gardenia dye diffused relatively slower although with stronger binding. To improve the photovoltaic conversion efficiency, a double layer of the two natural dyes extracted from gardenia and cochineal as sensitizers was successfully formulated on the nanoporous TiO_2 surface to harvest light over a wide range of wavelengths. The systematic studies of the adsorption equilibria and kinetics obtained in this work can be widely applied for other DSSCs based on natural products.

Acknowledgments

This research was supported by Specialized Local Industry Development Program through Korea Institute for Advancement of Technology (KIAT) funded by the Ministry of Trade, Industry and Energy, South Korea (1415127923 R0002040). This research was also supported by the Basic Science Research Program through the National Research Foundation of Korea (NRF), funded by the Ministry of Science, ICT and Future Planning, South Korea (NRF-2012R1A1A3010655).

References

[1] J.H. Yum, E. Baranoff, W. Wenger, M.K. Nazeeruddin, M. Grätzel, Energy Environ. Sci. 4 (2011) 842–857.
[2] M. Grätzel, Nature 414 (2001) 338–344.
[3] L.M. Peter, J. Phys. Chem. Lett. 2 (2011) 1861–1867.
[4] A. Yella, H.W. Lee, H.N. Tsao, C. Yi, A.K. Chadiran, M.K. Nazeeruddin, E.W.G. Diau, C.Y. Yeh, S.M. Zakeeruddin, M. Grätzel, Science 334 (2011) 629–634.
[5] F.G. Gao, A.J. Bard, L.D. Kispert, J. Photochem. Photobiol. A: Chem. 130 (2000) 49–56.
[6] H. Zhou, L. Wu, Y. Gao, T. Ma, J. Photochem. Photobiol. A: Chem. 219 (2011) 188–194.
[7] G. Calogero, J.H. Yum, A. Sinopoli, G.D. Marco, M. Gratzel, M.K. Nazeeruddin, Sol. Energy 86 (2012) 1563–1575.
[8] E.M. Abdou, H.S. Hafez, B. Bakir, M.S.A. Abdel-Mottaleb, Spectrochim. Acta A 115 (2013) 201–207.
[9] C. Sandquist, J.L. McHale, J. Photochem. Photobiol., A 221 (2011) 90–97.
[10] H. Chang, M.J. Kao, T.L. Chen, H. Guo, K.C. Choand, Z.P. Lin, J. Eng. Appl. Sci. 4 (2) (2011) 214–222.
[11] V. Shanmugam, S. Manoharan, S. Anandan, R. Murugan, Spectrochim. Acta A 104 (2013) 35–40.
[12] D. Zhang, N. Yamamoto, T. Yoshida, H. Minoura, Trans. Mater. Res. Soc. Jpn. 27 (2002) 811–814.
[13] K. Wongcharee, V. Meeyoo, S. Chavadej, Sol. Energy Mater. Sol. Cells 91 (2007) 566–571.
[14] A.S. Polo, N.Y.M. Iha, Sol. Energy Mater. Sol. Cells 90 (2006) 1936–1944.
[15] S. Hao, J. Wu, Y. Huang, J. Lin, Sol. Energy 80 (2006) 209–214.
[16] S. Ito, T. Saitou, H. Imahori, H. Ueharad, N. Hasegawa, Energy Environ. Sci. 3 (2010) 905–909.
[17] X.F. Wang, C.H. Zhan, T. Maeka, Y. Wada, Y. Koyama, Chem. Phys. Lett. 447 (2007) 79–85.
[18] R.Y. Ogura, S. Nakane, M. Morooka, M. Orihashi, Y. Suzuki, K. Noda, Appl. Phys. Lett. 94 (2009) 073308.
[19] K.T. Lee, S.W. Park, M.J. Ko, K.K. Kim, N.G. Park, Nat. Mater. 8 (2009) 665–671.
[20] Y. Ogomi, S.S. Pandey, S. Kimura, S. Hayase, Thin Solid Films 519 (2010) 1087–1092.
[21] K.H. Park, T.Y. Kim, J.Y. Park, E.M. Jin, S.H. Yim, J.G. Fisher, J.W. Lee, J. Electroanal. Chem. 689 (2013) 21–25.
[22] J. Li, H.A. Chase, Nat. Prod. Rep. 27 (2010) 1493–1510.
[23] K.H. Park, T.Y. Kim, J.Y. Park, E.M. Jin, S.H. Yim, D.Y. Choi, J.W. Lee, Dyes Pigment. 96 (2013) 595–601.
[24] M.E. Borges, R.L. Tejera, L. Diaz, P. Esparaza, E. Ibanez, Food Chem. 132 (2012) 1855–1860.
[25] T.Y. Kim, J.W. Lee, E.M. Jin, J.Y. Park, J.H. Kim, K.H. Park, Measurements 46 (2013) 1692–1697.
[26] A.W.M. Ip, J.P. Barfore, G. McKay, Chem. Eng. J. 157 (2010) 434–442.
[27] C.P. Hsu, K.M. Lee, J.T.W. Huang, C.Y. Lin, C.H. Lee, L.P. Wang, S.Y. Tsai, K.C. Ho, Electrochim. Acta 53 (2008) 7514–7522.